12-2019

Effects of Soil-Borne Pathogens on Seedling Establishment Patterns in Forest Systems

Eric P. Sodja
Utah State University

EFFECTS OF SOIL-BORNE PATHOGENS ON SEEDLING ESTABLISHMENT PATTERNS IN FOREST SYSTEMS

by

Eric P. Sodja

A thesis submitted in partial fulfillment
of the requirements for the degree

of

MASTER OF SCIENCE

in

Ecology

Approved:

Noelle Beckman, Ph.D. Major Professor	Luis F. Gordillo, Ph.D. Committee Member
Carrie A. Manore, Ph.D. Committee Member	Robert Schaeffer, Ph.D. Committee Member

Richard S. Inouye, Ph.D.
Vice Provost for Graduate Studies

UTAH STATE UNIVERSITY
Logan, Utah

2019

ABSTRACT

Effect of Soil-Borne Pathogens on Seedling Establishment

Patterns in Forest Systems

by

Eric P. Sodja, Master of Science

Utah State University, 2019

Major Professor: Dr. Noelle Beckman
Department: Biology

The Janzen-Connell mechanism is hypothesized to be an important contributor to maintaining plant diversity. It operates when species-specific natural enemies limit the density of their host species by seed consumption near parent tree locations. Soil-borne pathogens are a known contributor to this process, but the relative contribution of their life cycle stages are poorly understood. To determine the role of soil-borne pathogens in the development of Janzen-Connell recruitment patterns, we constructed a multi-scale simulation model of the interaction between tree populations and soil-borne pathogens. We characterized recruitment patterns based on the resulting spatial distribution of surviving seedlings and adult trees, and analyzed which attributes of plants and pathogens contributed to responses of tree and pathogen populations. Tree fecundity and seed dispersal distance were found to be the most important attributes determining tree populations and seedling density in relation to adult tree locations, while pathozone radius and oospores produced per infected host affected the locations and populations of pathogens. Pathogen effects on tree populations and seedling survivorship were not based on pathogen attributes, but instead on pathogen presence.

(61 pages)

PUBLIC ABSTRACT

Effects of Soil-Borne Pathogens on Seedling Establishment

Patterns in Forest Systems

Eric P. Sodja

The Janzen-Connell mechanism is proposed to maintain plant diversity: predators and diseases of seeds reduce the number of seeds that survive near a parent tree, but allow seeds far from the parent tree to grow into adulthood. In the area where seeds don't survive, seedlings from other tree species which are not affected by the seed consumer can grow. At large scales, this effect is thought to increase overall plant diversity. Soil-borne pathogens can contribute to seed mortality in this way, but we don't know how important different parts of their lifecycle are in creating Janzen-Connell patterns. To determine the role of soil-borne pathogens in the development of Janzen-Connell patterns, we constructed a simulation model to examine how tree and pathogen characteristics affect plant spatial patterns. Under specific combinations of tree and pathogen characteristics, we found that pathogens could create Janzen-Connell patterns. The most important parameters were how far trees dispersed their seeds, and how many seeds a tree produced in a year. These characteristics determined how much of an impact the pathogens were able to have on the tree population because they rely on the density of seeds to determine how far they can spread and how many spores they will produce.

ACKNOWLEDGMENTS

I would like to dedicate this thesis to my amazingly patient wife, Liz, who worked an extra two (plus) years at a crappy job so I could do this crazy thing. I'd also like to thank Dr. Beckman, who has provided patience, helpful learning experiences and useful advice from day one.

Eric P. Sodja

CONTENTS

LIST OF FIGURES

LIST OF STATE VARIABLES

Variable	**Interpretation**
$k(r)$	Probability of seed arrival at radius r
S	Living seeds
α	Pathozone coverage of cell
θ_P	Mean oospore infections per host
θ_Z	Mean zoospore infections per host
P_t	Active Oospores during t
R_I	Infected Root Presence
D	Dormant Oospores during f
S_M	Dead infected seeds
S_I	Living infected seeds
A_M	Number of dead trees
D_M	Dormant Oospore mortality
$Z_{t_{init}}$	Zoospores before dispersal
$m(l)$	Probability of zoospore arrival at radius l
Z_a	Zoospores arriving
Z_d	Zoospores departing
$Z_{t_{final}}$	Zoospores after dispersal

LIST OF PARAMETERS

Parameter	**Interpretation**	**Value Range**
σ	Dormant Oospore Mortality	$[0.75, 0.95]$
r	Pathozone Radius (m)	$[0.001, 0.1]$
c	Time steps t in f	4
μ	Zoospores Produced per Oospore	$[2, 15]$
ω	Oospores per Infected Host	$[1000, 1500000]$
q	Average Zoospore Dispersal Distance (m)	$[0.01, 10]$
ν	Infectivity	0.01
	Root Pathozone Coverage	100%
	Initial tree population	30
	Initial Tree Infection Proportion	0.3
δ	Infected Seed Mortality	0.9
γ	Adult Tree Mortality	0.0225
b	Seed Dispersal Shape Parameter	3
a	Seed Dispersal Scale Parameter*	$[-0.9, 5.54]$
e	Mean Seed Dispersal Distance* (m)	$[5, 125]$
j	Tree Fecundity	$[1000, 250000]$
	Background Seedling Mortality	0.5
ϵ	Spatial Cell Area (m^2)	25
	Spatial Sub-Cell Area (m^2)	0.01
	Spatial Cells in Model Space	3600

See appendix in section 3.3 for parameter range justifications.

*Seed dispersal scale parameter and mean distances are related by equation 1a.

CHAPTER 1

INTRODUCTION

Diversity is a fundamental attribute of ecological communities, but the mechanisms governing it are enigmatic. Various proposed hypotheses seek to explain observed patterns of diversity, such as heterogeneity in resource availability ratios, disturbance frequency, and the activity of natural enemies (Wright, 2002; Chesson, 2000). Natural enemies reduce the dominance of their host species in the system according to the abundance of host individuals. A common species can support a large population of natural enemies while rare species limit the natural enemies by being sparse. For natural enemies to promote diversity, they must limit the dominance of species when common and allow species to increase when rare (i.e. conspecific negative density dependence). Maintenance of species diversity by natural enemies can arise non-spatially (Mordecai, 2011). However, patterns of natural enemy attack and movement interact with patterns of seed dispersal. Hence, mortality of seeds and seedlings due to specialized natural enemies is a spatial process and can influence spatial distributions and diversity of plants as hypothesized by Janzen and Connell (Janzen, 1970; Connell, 1971).

The Janzen-Connell hypothesis assumes host-specific natural enemies suppress conspecific recruitment near mature seed-producing trees (Janzen, 1970; Connell, 1971). Spatial gaps in conspecific seedling recruitment develop near the seed-producing tree, allowing heterospecific individuals to establish. Survival probability of an individual seedling increases with increasing distance from the parent tree as natural enemy concentration declines. Seed arrival probability decreases with increased distance from the tree because seeds are more likely to disperse short distances. The resulting seedling recruitment probability peaks at an intermediate distance from the tree when seedling survival probability increases faster than the decrease in seed arrival probability (Janzen, 1970; Connell, 1971). It is hypothesized that the seedling recruitment gap establishes a minimum distance between conspecific individuals and therefore a minimum non-zero amount of open space wherein heterospecific individuals can establish (Janzen, 1970; Connell, 1971; Souza et al., 2013; Armstrong, 1989).

Other seedling recruitment patterns can develop depending on the interactions between natural enemies and hosts. The Hubbell pattern (Hubbell, 1980) occurs when seedling survival probability increases with increasing distance from the parent tree, but not enough to offset the declining probability of seed arrival. As a result, the establishment probability monotonically decreases with increasing distance – the peak in seedling recruitment is under the parent tree's canopy instead of outside it, as occurs in Janzen-Connell patterns. The McCanny pattern (McCanny, 1985) develops when survivorship decreases with increasing distance from the parent tree, which can arise through mechanisms such as seed consumer satiation near the parent tree or mutualistic interactions between the adult tree and its seedlings. This results in a more steeply declining survivorship curve than the Hubbell pattern, but a similar monotonically declining recruitment pattern emerges (Nathan and Casagrandi, 2004; Augspurger and Kitajima, 1992). Hubbell and McCanny patterns lack the gaps in seedling recruitment near the parent tree that are hypothesized to promote species diversity. Other seedling recruitment patterns, Exact Compensation and Invariant Survival, are intermediate cases between Janzen-Connell and Hubbell patterns, and between Hubbell and McCanny patterns, respectively. In Exact Compensation recruitment patterns, seedling recruitment is similar across distance because the increase in survivorship exactly offsets the decline in seed density due to seed dispersal patterns. Invariant Survival is the case where survivorship is similar across distance from the parent tree.

The seedling recruitment pattern resulting from natural enemy attack depends on the movement and consumption patterns of natural enemies in response to both local seed density and distance from the parent tree (Comita et al., 2014; Murphy et al., 2017). Natural enemies which rely on parent trees for some phase of their lifecycle tend to be distance-responsive seed consumers, searching for and consuming seeds within a limited distance of parent trees, while other natural enemies rely on and respond to the densities of seeds (Janzen, 1970). Even though the area with the highest seed density is often also closest to the parent tree (Bullock et al., 2017), under certain situations this may not be the case (e.g., under sleeping sites of spider monkeys, Russo et al., 2006) and can change the effect of natural enemy attack significantly (Beckman et al., 2012). The balance between how a natural enemy relies on distance or density of seeds determines

what seedling recruitment pattern will arise (Mari et al., 2008; Nathan and Casagrandi, 2004).

Insects, pathogens, and vertebrates have been identified as natural enemies that can cause Janzen-Connell patterns (Beckman et al., 2012; Fricke et al., 2014; Bagchi et al., 2014). The Janzen-Connell hypothesis bears an important assumption that natural enemies are host specific; otherwise, they consume seeds of other species that benefit from the recruitment gap near parent trees (Janzen, 1970; Connell, 1971; Sedio and Ostling, 2013). Host specificity is a spectrum, and those which are more host specific are thought to create Janzen-Connell effects most measurably; if not host specific, they at least are thought to have disproportionate effects across species (Augspurger, 1990; Liu et al., 2012), potentially depending on environmental conditions (Liu and He, 2019). Insects and pathogens have a higher degree of host specificity than vertebrates (Augspurger and Wilkinson, 2007; Konno et al., 2011), meaning that they should create Janzen-Connell patterns more strongly than vertebrates (Bagchi et al., 2014).

Soil-borne pathogens specifically, and especially oomycetes, have been identified as an important natural enemy for the Janzen-Connell hypothesis (Mordecai, 2011; Bever et al., 2015; Bagchi et al., 2014; Sarmiento et al., 2017). Oomycetes are widespread in natural systems (García-Guzmán and Morales, 2007) and have been shown to be important to patterns of seedling survival by causing high mortality rates among infected seedlings (Augspurger, 1983; Augspurger and Kelly, 1984; Neher et al., 1987; Gallery et al., 2007). Oomycetes respond to both distance from parent trees and density of potential hosts. In addition, infected tree roots support a population of pathogen spores continuously, allowing them to disperse spores season after season; infected trees effectively serve as a consistent source of pathogen spores (Liang et al., 2016). Local seed density determines the likelihood of spore arrival in that location resulting in successful infection of a seed – with more seeds in the location, infection by a given spore is more likely to occur. This moderates the ability of the pathogen to expand its range beyond the infected tree roots (Neher et al., 1987).

Beyond their response to seed density and distance from the parent tree, oomycete life cycles differ significantly from those of other commonly studied seed consumers,

such as insects (Beckman et al., 2012; Martin and Loper, 1999). Where insects have generation times on the order of weeks or months, oomycetes have generation times on the order of days which allows immediate population-level responses to changes in available resources and avoidance of local satiation (Martin and Loper, 1999). Thus McCanny patterns are unlikely with oomycete natural enemies (Beckman et al., 2012). They can also remain dormant for several months or sometimes years in unfavorable conditions until a viable host arrives (Augspurger and Wilkinson, 2007; Martin and Loper, 1999; Babadoost and Pavon, 2013). However, pathogens are severely limited in their dispersal capabilities, able to only disperse mobile spores millimeters through the soil (Martin and Loper, 1999; Heungens and Parke, 2000) where most insects are able to travel much longer distances in search of hosts.

Theoretical models of Janzen-Connell patterns typically include assumptions consistent with the life histories of insect or vertebrate natural enemies (Adler and Muller-Landau, 2005; Muller-Landau and Adler, 2007; Nathan and Casagrandi, 2004; Mari et al., 2008), but ignore the unique life-cycle characteristics of pathogens. Using a simulation study, Beckman et al. (2012) explored the importance of the differing life histories of insects versus pathogens for seedling recruitment patterns around one tree and found that the relative dispersal distances of seeds and natural enemies were important in identifying seedling recruitment patterns under both insect seed predation and pathogen attack. For pathogens, they found spores with much shorter dispersal distances compared to seeds could still track seeds through space with their ability to remain dormant in the soil; spore effectiveness in tracking seeds depended on pathogen fecundity, seed dispersal, and spore dispersal (Beckman et al., 2012).

While this is an important advance in our understanding of the potential role of differing life history strategies of natural enemies for plant spatial patterns, their model focused on one tree, one spore type (that had both the ability to disperse through the soil and remain dormant in the soil), and did not investigate how varying degrees of spore dormancy influence spatial patterns for a population of plants. In this study, we developed a spatially-explicit simulation model to examine how aspects of pathogen life history influence seedling recruitment patterns. Specifically, we investigate the influence

of zoospore dispersal, oospore dormancy, and the size of the spore pathozone on seedling recruitment patterns for a simulated population of plants.

CHAPTER 2

METHODS

2.1 System Overview

We model a population of plants over several years. At the beginning of each fruiting season, plants disperse their seeds. Trees rely on many mechanisms for seed dispersal, including wind and animal dispersal (Nathan et al., 2012). In this model, we used a dispersal kernel that fits both mechanisms of dispersal reasonably well (Clark et al., 1999; Muller-Landau and Adler, 2007). After dispersal, emerging seedlings were subject to mortality from pathogen infection and competition from other seedlings and adult trees. Infected trees operated as long-term sources of pathogen spores from infections on their roots.

Oomycetes have two types of spores, oospores and zoospores (Martin and Loper, 1999). Oospores are sessile and have active and dormant states, while zoospores are mobile (Martin and Loper, 1999; Latijnhouwers et al., 2003). Active oospores which have successfully infected a host tree root or seedling produce zoospores in large quantities. Dormant oospores, defined as those which are not currently infecting a host root or seedling, do not produce zoospores but are able to remain living for long periods of time, sometimes several years or decades (Martin and Loper, 1999; Babadoost and Pavon, 2013). Dormant oospores become active when chemical signals of a germinating seed or growing root are detected, in response to which they grow hyphae in the direction of the signal and begin production of zoospores (Martin and Loper, 1999; Latijnhouwers et al., 2003). Zoospores are the primary means of spatial spread by pathogens. However, zoospores have very short lifespans; their abundance at any given time relies directly on the productivity of active oospores (Martin and Loper, 1999). When a zoospore finds a host, infection occurs and oospores are produced (Latijnhouwers et al., 2003).

The interaction between seeds and pathogens is based on the *pathozone*, the area wherein a pathogen spore can effectively detect and infect a host (Gilligan, 1985; Bailey and Gilligan, 1999; Gilligan and Bailey, 1997). The size of the pathozone is determined

by the ability of the fungal hyphae to reach the host; we have assumed both zoospores and oospores interact with hosts through pathozones of equal size.

2.2 Model Description

2.2.1 Space and Time

The different distances of dispersal posed a modeling challenge; trees disperse seeds over tens to thousands of meters, while oomycete pathogens can only disperse spores as far as a few centimeters at the maximum (Heungens and Parke, 2000; Bullock et al., 2017; Rekah et al., 2007; Bailey et al., 2005). Seeds and pathogen populations were modeled in square spatial cells 5 by 5 meters in size, which is the average crown area for reproductive trees on Barro Colorado Island in Panama (O'Brien et al., 1995; Bohlman and O'Brien, 2006; Muller-Landau et al., 2006). This area also represented the root extent of the tree where pathogens could infect tree roots, and the area where an infected adult tree supported a population of pathogen oospores. The spore interactions with seeds and roots took place in 0.1 by 0.1 meter "sub-cells" inside these larger spatial cells. Seeds were infected by pathogens in these sub-cells, but competed with other seeds and adult trees within the larger ($5m^2$) cells. The total simulation space was set at 9 hectares to capture the dynamics of a potentially large tree population while balancing computational resources needed to run a sufficient number of simulations in a reasonable amount of time.

The difference between the timing of the life stages of pathogens and trees was an additional challenge to modeling their relationship effectively. Seed dispersal occurs annually from mature adult trees, i.e. seedlings that survived the previous seed dispersal season and have matured, as well as existing adult trees. Pathogen reproduction cycles complete within hours or days, and therefore can occur several times between seed dispersal events (Martin and Loper, 1999). The temporal differences in pathogen and tree life cycles required two different timescales, which we designated t and f. Pathogen life cycles occurred in each time step t, c of which were contained within each reproductive cycle for trees, denoted by time step f (essentially, the length of f was t times c). We based this framework on the assumption that trees and pathogens both follow reproductive cycles synchronized to other individuals in their populations, which exchanged a reduction in model realism for simplified data interpretation and a reduction in the computational resources required to run the model.

The notation for time in this paper is based on subscripts of f and t on state variables. For example, hypothetical state variable X during the previous time step $f-1$ is given by X_{f-1}. If additional subscripts are used, they modify the state variable to indicate a subset of it. Subset Y of X during $f-1$ would be $X_{Y,f-1}$. When a subscript t is used, f is always the current seed cycle time step f (as opposed to $f-1$, the previous seed cycle time step). For tables of state variables and parameters with their meanings, see section 3. The state variables within spatial cells are independent of one another aside from seed and zoospore dispersal.

2.2.2 Starting Conditions

Initially, the model randomly distributed a starting population of 30 trees in the simulation space by sampling x and y coordinates from a uniform distribution. Each of these initial trees had a 30% probability of initial infection, which was applied using a Bernoulli trial for each tree with a chance of success of 30%. There were no pathogen spores initially present, but during the first t time step the roots of the initially infected trees produced oospores, which in turn produced zoospores. There were no dormant oospores until the end of the first t time step.

2.2.3 Seed Dispersal

Each adult tree in the system produced the same number of seeds and dispersed them equally in every direction at a distance according to a bivariate Student's t distribution (or "2Dt") dispersal kernel (Clark et al., 1999; Nathan et al., 2012):

$$k(r) = \frac{(b-1)}{\pi a^2}\left(1+\frac{r^2}{a^2}\right)^{-b} \tag{1}$$

where b is the dispersal shape parameter (degrees of freedom), a is the distance parameter, and r is the radius. In accordance with previous models (Beckman et al., 2012; Muller-Landau et al., 2008), the shape parameter was set to 3 for all simulations. Mean dispersal distance (e) for the 2Dt kernel is

$$e = \frac{\pi}{2}\exp\left(\frac{a}{2}\right) \tag{1a}$$

(Muller-Landau et al., 2008; Beckman et al., 2012).

The probability of seed arrival for each cell was found by integrating this dispersal kernel across the cell area, and then normalizing the probabilities of all the cells by dividing the probability for each cell by the total probability for the calculated dispersal kernel area. The expected number of arriving seeds in a cell from a given tree was the number of seeds dispersed per tree times the normalized value of $k(r)$ for that spatial cell. This expected dispersal matrix was repeatedly copied and centered on each tree in the simulation space, and the values in each cell of the stacked matrices were summed according to their coordinates to obtain a total number of expected seeds to be dispersed to each spatial cell. The number of seeds actually arriving in a cell was drawn from a Poisson distribution with mean (λ) equal to the sum of the expected number of seed arrivals from all contributing source cells.

Any seeds dispersed farther than the edges of the simulation space were adjusted by a torus function to simulate the arrival of seeds from outside the simulation space. This assumed that the simulation space was surrounded by forest with the same properties as the simulated space, and therefore avoided edge effects.

2.2.4 Pathozone

A *pathozone* is the area surrounding a potential host in which a spore is able to detect and infect a potential host seed or root, and was the basis of the spatial pathogen-host interactions in this model. We assumed that seeds and pathogens were distributed randomly within a spatial cell, so the proportion of the cell covered by a pathozone determined the likelihood that a spore and host would interact. For example, if pathozones covered 25% of the cell, a spore dispersing to the cell had a 25% chance of landing within that collective pathozone, and therefore had a 25% chance that it would have the opportunity to infect a host. Pathozones were circular with radius r, the maximum distance from a host that they could cause an infection.

The proportion of a spatial cell covered by a single host's pathozone was calculated by

$$\alpha = S\frac{\pi r^2}{\epsilon} \tag{2}$$

where α is the proportion of the cell covered by the pathozone, r is the radius of the

pathozone measured from the center of the seed, and ϵ is the area of the spatial cell, 25 square meters in this version of the model. We also used α to calculate the proportion of dormant oospores activated by arriving seeds or new roots (see equation 5c).

We assumed that any spore has the opportunity to infect at most one host, and the pathozone for each host was small enough that it would not overlap other hosts' pathozones until the entire cell was covered by the pathozones for a given type of spore. Under these circumstances, the proportion of the cell covered by the cell's collective pathozone became 100% regardless of the number of potential hosts in the cell above this maximum level. All potential hosts in the cell encountered a pathogen spore and could have been infected, assuming the pathogen had enough spores in the cell to have at least one encounter with each potential host. Hosts could therefore have a large number of spores attempting to infect them during each time step t.

Roots had a very large pathozone, covering the entire spatial cell where the tree was located. Any spore landing in a cell where roots were present interacted with those roots (i.e. α for the roots was equal to 1), though infection did not necessarily occur.

2.2.5 Infection

Infection was based on the number of interactions between spores and potential hosts, determined by the pathozones described in section 2.2.4 and the probability of a spore germinating and infecting a seedling, or *infectivity*. The presence of roots, R, within each spatial cell took a value of 0 (when no tree was present) or 1. Roots within a cell were considered either all infected or uninfected, with the infected roots in a cell producing ω oospores during each time step t. We assumed a cell of infected roots produced the same number of oospores as a single infected seed. The oospores infecting roots maintained their active production of zoospores as long as the tree associated with those roots was alive.

The expected number of successful infections (θ) depended on the infectivity coefficient (ν), the number of spores (P), and the proportion of the spatial cell covered by

the pathozone (α). The expected number of successful infections per host was

$$\theta = \frac{\nu\alpha P}{S}, \tag{4a}$$

We assumed that seeds, including those which were already infected, could be targeted by multiple zoospores and/or oospores in a single time step t. Previously infected seeds absorbed some of the infectious spores in the cell, creating diminishing returns on expected successful infections for each additional spore added to the cell.

The probability of at least one successful infection of a given seed during a time step t was based on the probability that a seed would *not* be infected, with X as the number of successful infections of an individual seed:

$$Pr(X > 0) = 1 - (1 - \nu\alpha)^P$$

Assuming the number of spores P is large and the probability of infection $\nu\alpha$ is small, this probability can be approximated by

$$Pr(X > 0) = 1 - e^{-\theta}. \tag{4b}$$

The number of seeds infected during each time step t was drawn from a binomial distribution with the probability given by equation 4b.

The same framework was implemented for roots, but with $\alpha = 1$ signifying complete coverage of the cell by the root pathozone.

2.2.6 Oospore Populations

Oospore population calculations had to be modified between the first time step t in f ($t = 1$) and those that came after ($t > 1$). During each first time step t in any time step f, there were no infected seeds and all oospores were either from infected roots (whose oospores were always active) or dormant oospores that had been activated by seeds landing near them:

$$P_{t=1} = \omega R_I + \alpha D_f \tag{5a}$$

where $P_{t=1}$ is the number of active oospores in time step $t = 1$, ω is the number of oospores produced per infected host, R_I is the infection status of roots in the cell (I has a value of either 0 or 1, for roots absent or uninfected [$I = 0$], or present and infected [$I = 1$]), D_f is the number of dormant oospores in the cell from the previous time step f, and α is the proportion of the cell covered by the total pathozone of all seeds (calculated in equation 2).

For $t > 1$, the total active oospores was the sum of oospores from the infected roots and seeds, minus those from seeds that died from infection in previous time steps t, as their oospores would become dormant:

$$P_{t>1} = \omega \left[R_I + \sum_{i=1}^{t} (S_{I,t=i} - S_{M,t=i}) \right] \tag{5b}$$

where $S_{I,t=i}$ is the number of infected seeds in time step $t = i$ (including all infected seeds surviving during t), $S_{M,t=i}$ is the number of seeds that died during time step $t = i$, and ω is the number of oospores produced per infected host.

All active oospores were assumed to expend their available resources by production of zoospores and die during t; they were replaced by new oospores in the cell if more hosts were successfully infected. Oospores from infected tree roots were included in $t > i$ time steps because the activated oospores were assumed to have a consistent (but limited) supply of resources provided by the tree and therefore persist between time steps t. Dormant oospores were only included in equation 5a and not equation 5b because they could only be activated by arriving seeds, which occurred at the beginning of f before $t = 1$, or maturing trees, which only occurred at the end of f after time step $t = c$.

The number of dormant oospores for a given time step t depended on previously dormant oospores that had *not* been activated by new seed arrivals, and dormant oospores from seeds that died in the previous time step:

$$D_t = (1 - \alpha) D_{f-1} + \omega \sum_{i=1}^{t} S_{M,t=i} \tag{5c}$$

where D_t is the number of dormant oospores for time step t.

The number of dormant oospores that died at the end of f is $D_{M,f}$. In this model, the duration of oospore survival while dormant had no set upper limit. At the end of each time step f, however, each dormant oospore was subject to death with probability σ which was applied as the probability of success in a binomial trial to determine how many dormant oospores survived in each cell. Total dormant oospores at the end of f was given by

$$D_f = D_{t=c} + \omega R_I A_{M,f} - D_{M,f} \tag{5d}$$

where $A_{M,f}$ was the number of trees that died during f (see section 2.2.8).

2.2.7 Zoospore Populations and Dispersal

Zoospore populations at the beginning of any time step t started at zero because their lifespan was equal to the time period represented by t. Their abundance during t was determined by the number of zoospores produced by active oospores in the cell:

$$Z_{t_{init}} = \mu P_t \tag{6a}$$

where $Z_{t_{init}}$ is the number of zoospores produced in the cell during time step t and μ is the number of zoospores produced for each active oospore, P_t. To model spore dispersal, we used a negative exponential function:

$$m(l) = \frac{1}{2\pi q^2} exp\left(- \frac{l}{q} \right) \tag{6b}$$

where $m(l)$ is the probability that the dispersed spore will land at distance l, and q is the dispersal distance parameter. The mean dispersal distance (m) is $2q$.

In order to save computational resources, we pre-calculated a matrix of the expected number of zoospores dispersed from a focal cell for each value of q. The probability of zoospore dispersal out of the cell was based on dispersal from 0.1x0.1 m sub-cells within the 5x5 meter spatial cell. Dispersal probabilities were calculated from each sub-cell, and the overlapping matrices of dispersal probabilities were summed together. This dispersal probability was normalized so that the entire dispersal from all sub-cells summed to 1, and then multiplied by μ to find the expected number of zoospores dispersed from the

5x5 meter cell from one active oospore, similar to the procedure described in section 2.2.3 for seed dispersal calculations. This resulted in a 3x3 cell matrix which was then centered on each 5x5 meter cell in the simulation space where active oospores were present, and multiplied by the number of active oospores in the central cell; any overlapping cells from the 3x3 matrices were added together to obtain the expected number of total zoospores per cell. The torus function was applied to allow spores dispersed over the edge of the simulation landscape to land in the cells on the opposite edge of the landscape. The result was a matrix covering the entire simulation space of the expected number of zoospores in each location. The final number of zoospores present in a cell was drawn from a Poisson distribution with the expectation equal to the expected number of total zoospores in each cell from oospore generation as well as dispersal from neighboring cells.

2.2.8 Seed and Tree Mortality

At the end of time step t, all seeds which had been infected by pathogens were subject to a probability of mortality. The number of seedlings that died due to infection was drawn from a binomial distribution with a high probability of mortality ($\delta = 90\%$). If an infected seed died, it left behind ω dormant oospores that were added to D_t (see equation 5c). All seedlings were also subject to a background mortality rate of 50%, regardless of their infection status. The number of seedlings that died was drawn from a binomial distribution with a probability of mortality of 50%.

If the 5x5 meter cell was not occupied by an adult tree, a surviving seedling would mature into an adult. In the presence of an adult tree, any surviving seedling in that cell died due to competition. If the dying seedlings were infected, they left behind dormant oospores (handled in equation 5d). Seedlings were assumed to compete for resources within a spatial cell, and only one seedling in each cell could mature into an adult. The infection status of this surviving seedling was determined by the proportion of infected seedlings in the cell, applied as the probability of success when drawing from a binomial distribution:

$$Pr(Y = 1) = \frac{S_{I,t=c}}{S_{t=c}} \tag{7}$$

where Y is the outcome of the binomial trial (value of 0 or 1), $S_{I,t=c}$ is the number of

infected seeds in the cell during the previous time step t, and $S_{t=c}$ is the number of seeds in the cell (infected and uninfected) during the previous time step t. An infected maturing seedling had infected roots for the rest of its life.

Each adult tree was subject to a probability of mortality. Tree mortality was independent of infection, and was applied by sampling a Bernoulli trial with probability $\gamma = 0.0225$ for each adult tree (based on empirical observations from BCI by Condit et al., 2017; see section 3.3). If the dying tree was infected, the oospores on its roots became dormant and were added to D_f. The number of trees that died during f was given by $A_{M,f}$ (see equation 5d).

2.3 Simulations and Analysis

Simulations were run using 500 unique input parameter combinations sampled from the parameter ranges in table 3 using the Latin Hypercube generating function in the 'spartan' R package (Alden et al., 2018). The size of the simulation space was 60 by 60 cells (300 by 300 meters), or 3600 total cells. Simulations were run until the simulation space reached a maximum number of adult trees (3600) or 500 seed dispersal seasons, whichever came first.

2.3.1 Identifying Seedling Recruitment Patterns

Seed dispersal patterns were categorized into recruitment patterns based on the location of maximum surviving seedling densities (under canopy cover or not) and the difference between survivorship under the tree canopy versus outside of canopy cover, both calculated before seedling mortality due to competition from intraspecific adults or seeds was applied (Beckman et al., 2012). All cells in the simulation space were identified as belonging to one of a series of annuli based on their distance from the nearest adult tree (Fig. 2.1). Initial seed and surviving seedling densities were calculated for each of the annuli by dividing the total number of seeds/seedlings in the annulus at each distance from parent trees by the total area of the annulus. Within each annulus, the number of surviving seedlings was divided by the number of initial seeds to calculate survivorship per annulus.

If maximum surviving seedling density was at a distance outside of the parent crown, the magnitude of the difference between the maximum and minimum surviving seedling density was compared by calculating the relative difference:

$$\text{Density Difference} = \left| \frac{\max(\text{Seedling Density}) - \min(\text{Seedling Density})}{\max(\text{Seedling Density})} \right|$$

If the relative difference between them was greater than 0.1, the seed dispersal pattern was classified as Janzen-Connell. If not, the recruitment pattern was Exact Compensation.

If maximum surviving seedling density was under the parent crown, the recruitment pattern could be Hubbell, McCanny, or Invariant Survival, depending on the shape of

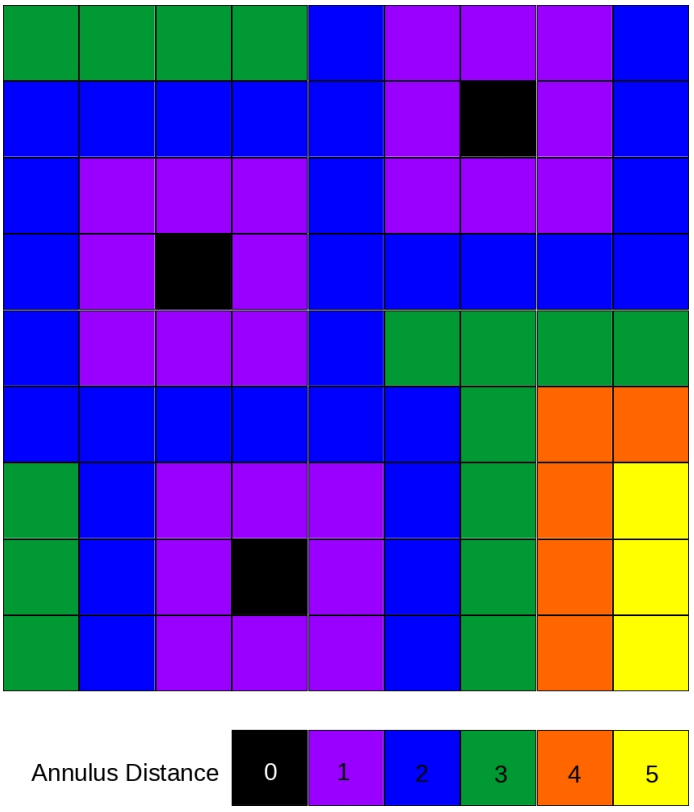

FIGURE 2.1: Example annuli for tree populations. Adult trees are in the black cells.

the survivorship curve. This was calculated by comparing the survivorship under the canopy with the maximum survivorship outside the canopy:

$$\text{Survivorship Difference} = \frac{\max(\text{Surv. Under Canopy}) - \max(\text{Surv. Outside Canopy})}{\max(\text{Survivorship})}$$

Survivorship differences greater than 0.1 were classified as Hubbell patterns, less than -0.1 were McCanny patterns, and values between -0.1 and 0.1 were Invariant Survival.

2.3.2 Tree/Seedling Analysis

We used decision trees to analyze the importance of plant and pathogen attributes for classifying seedling recruitment patterns, seedling survivorship, the number of trees

at equilibrium, and the distance between peaks in seedling recruitment density and nearby adults. As trees in 359 of the 500 simulations saturated the landscape before the 500th season, we also analyzed the number of seed dispersal seasons until the simulated landscape was either saturated with adult trees or the simulation reached 500 seasons, whichever occurred first. For each decision tree, we included death rate of dormant oospores (σ), average dispersal distance of zoospores (q) and seeds (e), pathozone radius (r), tree fecundity (j), and the ratio between seed and zoospore dispersal distance ($e : q$) as explanatory variables. The decision trees shown in figures required at least 20 observations remaining at a node for a split to be attempted. All regression and classification trees were conducted with the rpart package for R (Therneau and Atkinson, 2018) with default settings.

A classification tree was used to analyze seedling recruitment patterns identified during the last season of each simulation. Seedling survivorship was analyzed using a regression tree analysis, with survivorship calculated as the total number of seedlings divided by the number of seeds in the last season of each simulation for the entire simulation space. We also used regression tree analysis to analyze the number of seasons until the simulation space was saturated with adult trees, and the number of trees at equilibrium.

In addition, we analyzed the average distance between adult trees and peaks in surviving seedling density at a local scale (Fig. 2.2) before seedling mortality due to factors besides pathogen attack was applied. A cell was identified as a local peak if it had more surviving seedlings than the 8 spatial cells immediately surrounding it. Each seedling density peak's nearest adult tree was identified, allowing each peak to contribute to the average peak-tree distance for the whole simulation space, even if another seedling density peak was closer to the nearest adult tree. The average distance found for each simulation's last season was used as the response variable in the regression tree analysis.

2.3.3 Pathogen Analysis

Pathogen oospores were analyzed for their overall population size, the relationship between pathogen and seed densities, distance of peaks in pathogen density from adult trees, and distance of pathogen oospores from the nearest tree. Zoospores were not

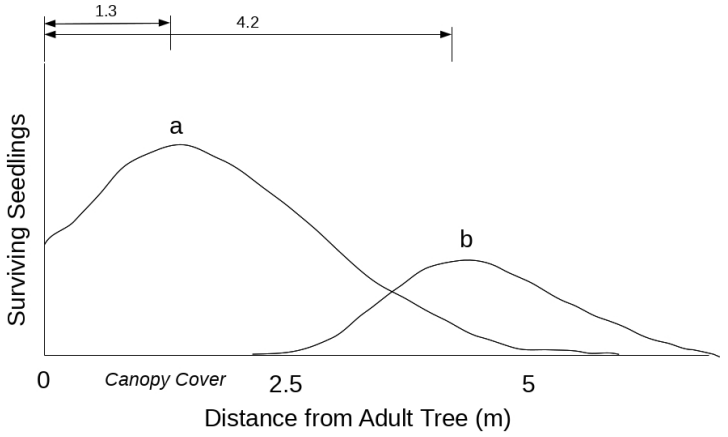

FIGURE 2.2: Tree-seedling density peak distance diagram. Recruitment patterns are classified as Janzen-Connell if the peak of the surviving seedling density curve is outside of the canopy crown; otherwise, it is classified as McCanny, Hubbell, or Invariant Survival, depending on the shape of the survivorship curve.

analyzed because their abundance and location were directly related to the number of oospores. Pathogen oospore patterns were analyzed using the same types of decision trees and explanatory variables as those used for analyzing tree and seed patterns.

The overall population of oospores was analyzed at the end of each simulation to get the number of oospores in the system when the tree population reached equilibrium. Pathogen and seed densities were compared on a cell-by-cell basis by dividing the number of oospores in each cell by the number of seeds in the same cell. This measure of oospores per seed was then averaged across cells for the last season in each simulation. The distance between peaks in oospore density and the nearest adult tree was calculated using the same process as that used to calculate local peaks of seedling density, as described above. Finally, the distance of each spore to the nearest tree was calculated, and the overall distance was averaged for the entire simulation space to compare the distance pathogen oospores were able to establish away from adult trees.

Additionally, we analyzed changes in these response values from the first to the last spore dispersal season during the last seed dispersal season in each simulation using

decision trees. To understand the overall response of pathogens we analyzed pathogen responses (e.g. spore abundance) during the first spore season of the final seed dispersal season of the simulation. To understand the dynamics of the spores, we analyzed the difference between the first and last spore seasons (e.g. the absolute value of the spore abundance during the first spore cycle minus the spore abundance during the last spore cycle in the season).

CHAPTER 3

RESULTS, DISCUSSION, AND CONCLUSION

3.1 Results

3.1.1 Seedling and Tree Patterns

In 359 out of the 500 simulations, the landscape became saturated with trees, that is, all 3600 cells of the simulation landscape were occupied by one adult tree each before the 500th dispersal season (the maximum number of seasons for simulations). For these simulations, the number of seasons until tree saturation ranged from 1 to 460. Regression tree analysis indicated that tree fecundity and average distance of seed dispersal were the most important factors contributing to the number of seasons until saturation (Fig. 3.1). In simulations where trees had low fecundity or moderate average seed dispersal distance (i.e., dispersal distances ranging from 7.2 to 8.5 meters), trees saturated the simulation space only after hundreds of seasons, if at all. In simulations with high fecundity ($> 65,000$) and seed dispersal outside the range previously mentioned, trees saturated the landscape in 120 dispersal seasons or fewer.

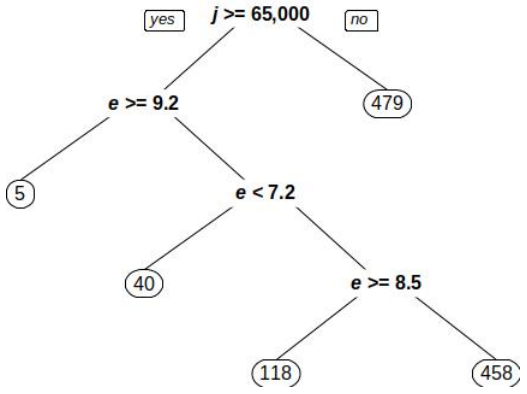

FIGURE 3.1: Time to adult saturation.

The seedling recruitment patterns observed in the simulations were divided among Janzen-Connell (26%), Hubbell (35%) and McCanny (38%), with the remaining 1% split between Exact Compensation and Invariant Survival. A classification tree analysis was conducted for recruitment patterns in the last season of each simulation (Fig. 3.2). Tree fecundity and seed dispersal distance had a significant effect, especially in developing Janzen-Connell patterns, while oospore fecundity, pathozone radius, and the ratio between seed and zoospore dispersal distances differentiated between Hubbell and McCanny patterns. Janzen-Connell patterns were found at low tree fecundities ($j < 9000$) or moderate seed dispersal distances at high tree fecundity ($7.6 < e < 8.2$).

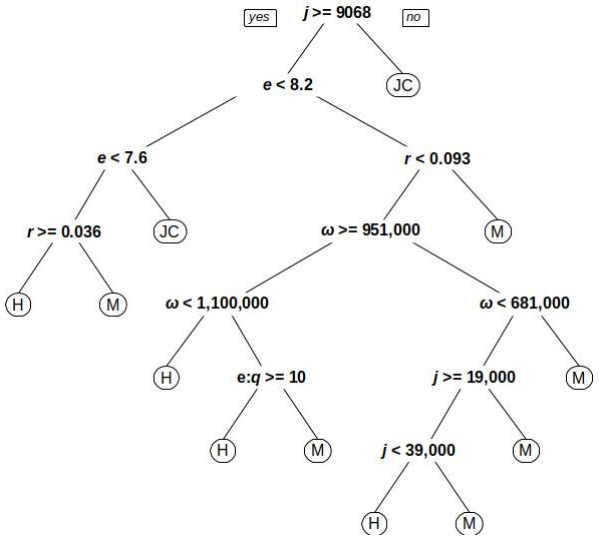

FIGURE 3.2: Seedling recruitment pattern classification tree.

Overall seedling survivorship ranged between 0 and 0.26 across simulations, with a median value of 0.004. According to our regression tree analysis, the overall survivorship of seedlings during the last season of each simulation was influenced by tree fecundity (Fig. 3.3). Seedling survivorship was four times higher when tree fecundity was above 11,000 seeds per tree per dispersal season, compared to when fecundity was below 11,000.

The distance between adult trees and local peaks in surviving seedling density was influenced by both tree fecundity and mean seed dispersal distance (Fig. 3.4). Increasing

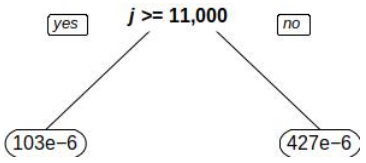

FIGURE 3.3: Survivorship of seedlings.

fecundity resulted in decreases in average tree-peak distance, with a maximum average distance of 15 meters when fecundity was less than 11,000. At fecundity levels greater than 21,000 seeds per tree, average seed dispersal distances between 7.5 and 8.3 meters resulted in a greater average distance between seedling peak densities and adult trees (4.1 meters) than did seed dispersal distances outside that range (0.12 to 0.32 meters).

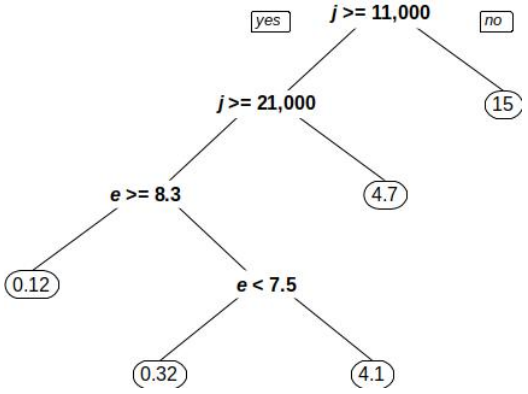

FIGURE 3.4: Tree-seedling density peak distance.

The number of trees at equilibrium ranged from 57 to 3600, with a median at 3600 and a mean of 3318. Based on the regression tree analysis, the number of trees in the landscape at equilibrium depended on tree fecundity, seed dispersal distance, and pathozone radius (Fig. 3.5). Higher tree abundances were reached when tree fecundity was relatively higher and oospore pathozone radius was smaller. Tree abundances were

lower when average dispersal distances of seeds were intermediate (between 7.5 and 8.3 meters).

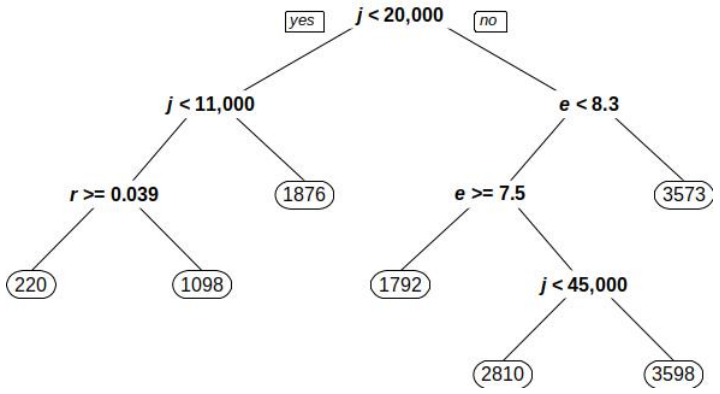

FIGURE 3.5: Adults at equilibrium.

3.1.2 Pathogen Patterns

By the last seed dispersal season of the simulations, the number of cells occupied by oospores ranged between 58 and 3600. The average number of cells occupied was 3407, while the median was 3600. More complete coverage of the simulation space by oospores was observed with seed dispersal distances higher than 8.5 meters and less than 7.5 meters, especially with lower tree fecundity (Fig. 3.6).

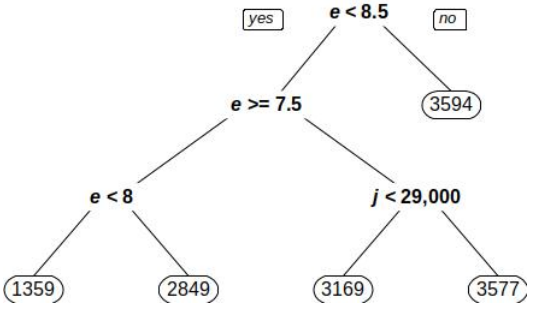

FIGURE 3.6: Cells occupied by oospores.

The difference in the number of cells occupied by oospores during the last season of each simulation showed that tree fecundity and seed dispersal distances were important factors, and oospore fecundity (zoospores produced per oospore) also affected these patterns. Higher levels of tree fecundity helped keep the pathogen presence more stable (i.e. there were smaller changes in the number of cells occupied). Lower fecundity allowed for larger difference in cell occupation by oospores, while larger oospore fecundities and smaller seed dispersal distances moderated changes in the number of occupied cells when fecundity was below 11,000 (Fig. 3.7).

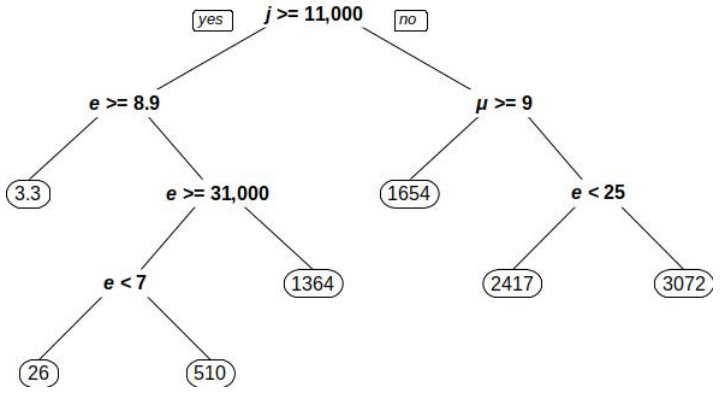

FIGURE 3.7: Changes in cells occupied by spores. Change is between first and last spore cycles of final season of all simulations.

The total number of spores divided by the number of seeds in each cell, averaged over the first spore dispersal cycle of the last seed dispersal season of each simulation, showed that spores are generally more capable of tracking seed dispersal when oospores produced per infected host and pathozone radius are large and seed dispersal distance is small (Fig. 3.8).

The difference between the pathogen to seed ratios at the beginning and end of the final season showed that most of the same parameter combinations that contributed to the seed-oospore ratios in the first place also caused the ratio of pathogens to seeds to change dramatically (Fig. 3.9). High seed dispersal distance (more than 49 meters), with high number of oospores produced per infected host (greater than 792,000) and

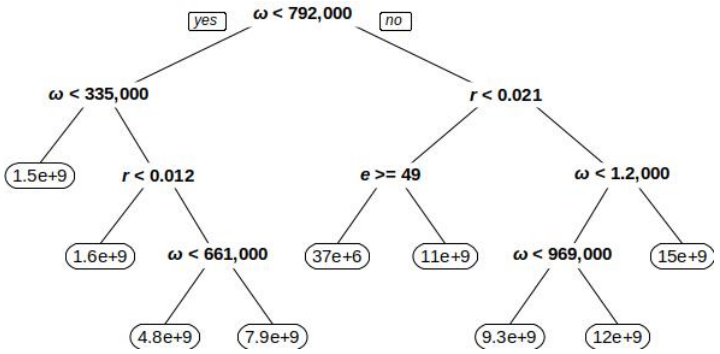

FIGURE 3.8: Average number of spores per seed.

small pathozone radius (less than 0.021 meters) resulted in a much smaller change in the spore to seed ratio than was observed from other parameter combinations. Most of the responses in figures 3.8 and 3.9 are the same for the values shown (though they differ in small amounts in the digits not displayed) while the parameter combination that includes high seed dispersal distance shows a difference of approximately 9 million. That is, this parameter combination resulted in 9 million spores per seed left by the end of the spore dispersal season, a much higher proportion of the original seeds than was observed with any other parameter combination (though other parameter combinations resulted in several orders of magnitude greater ratios of spores to seed to begin with).

The distance between the peaks of spore density and adult trees showed a wide range of values, from as little as 4 meters to as high as 26 meters on average (Fig. 3.10). At tree fecundity above 11,000, pathozone radius above 0.099 resulted in higher distances, while fecundities above 20,000 with pathozone radius less than 0.099 resulted in the lowest overall distances. Lower tree fecundities than 11,000 resulted in higher tree-peak distances and the combination of low fecundity and high dispersal of seeds resulted in the farthest overall distance. Low fecundity and lower distance allowed pathozone radius to differentiate between moderate (11m) and moderately high (21 m) distance.

The change in the distance between the peaks of pathogen density and adult trees

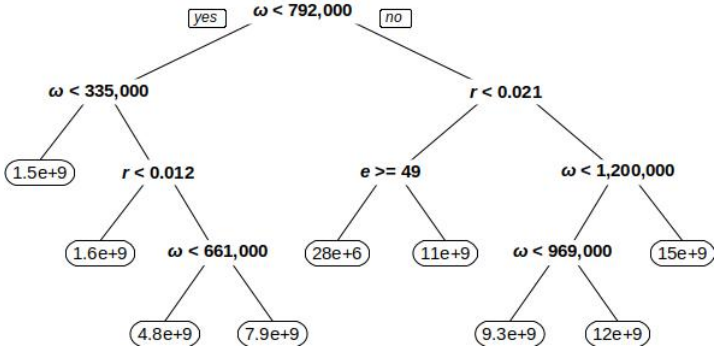

FIGURE 3.9: Change in seed/oospore ratio.

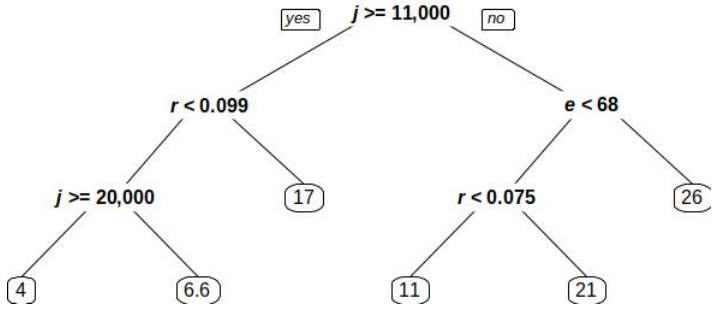

FIGURE 3.10: Distance between peaks in spore density and adult trees.

showed that tree fecundity was again a primary dividing variable (Fig. 3.11). Simulations with low tree fecundities (approximately 10,000 or less) allowed dormant oospore mortality to influence the change in distance, with a smaller change resulting from higher mortality. Larger changes were the result of larger tree fecundities.

The average distance of each oospore to the nearest adult tree was determined by tree fecundity, seed dispersal distance, and oospore fecundity, with lower tree fecundity creating larger distances, and higher seed dispersal distance causing higher average distances for simulations with tree fecundity above 11,000 (Fig. 3.12). Oospores produced

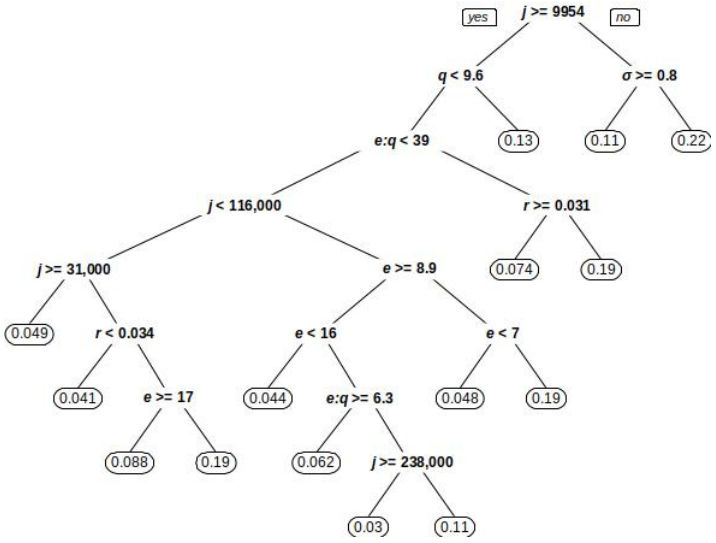

FIGURE 3.11: Change in spore peak density to tree distance.

per infected host only applied at low fecundity and higher dispersal distance, and created only a minor (4 m) difference in average distances.

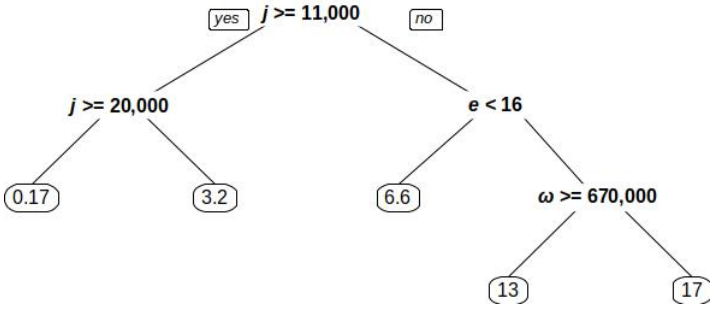

FIGURE 3.12: Distance between oospores and trees.

The change in average oospore distance from adult trees over the course of the last seed dispersal season was driven primarily by tree fecundity (Fig. 3.13). Simulations with higher tree fecundity had less change in oospore distance than those with fecundity

less than about 9,600. Oospores per infected host was important with lower tree fecundity, and a lower number of oospores per infected host created larger changes in average distance. Seed dispersal distance was an important variable in simulations with higher fecundity, and generally higher seed dispersal distance resulted in smaller changes in the distance between oospores and trees.

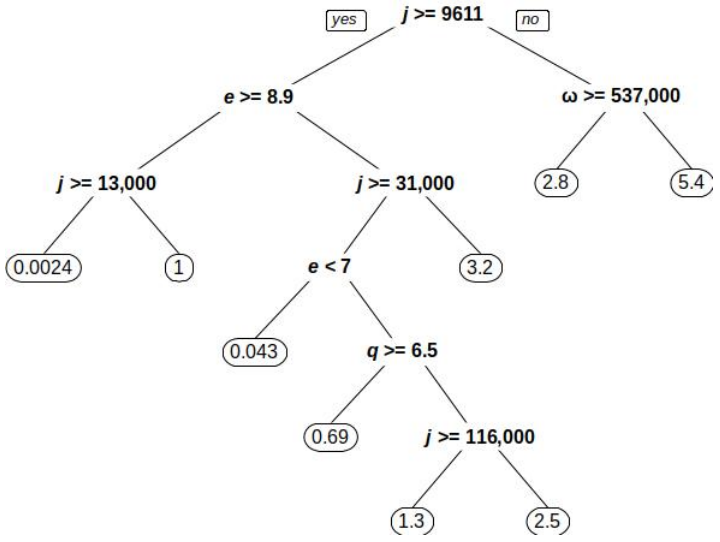

FIGURE 3.13: Changes in oospore to tree distance.

3.2 Discussion

Using a simulated population of plants and their pathogens, we explored how life history strategies of pathogens influence spatial patterns of their plant hosts. Measurements of seed and tree attributes such as seedling recruitment patterns, equilibrium number of trees, seasons to saturation, and the distance between peaks in seed density and adult trees all indicated that tree fecundity and seed dispersal distance were the primary factors influencing tree population patterns. Measurements of pathogen activity indicated that tree fecundity was also a primary influence on pathogen activity, but pathogen attributes played a stronger role, especially the number of oospores produced per infected host.

3.2.1 Seed Dispersal Counteracts Fecundity

Among many of the regression trees that tested the responses of the tree population, the range of seed dispersal distance from approximately 7.2 to 8.5 meters arose multiple times (Figs. 3.2, 3.1, 3.4, 3.5). The reason that we see this pattern may have to do with the prominence of a pathogen effect. With high tree fecundity and low seed dispersal distance, there will be many seeds close to the tree – so many that even pathogens, which reproduce quickly in very large numbers, may not be able to cause mortality sufficient to create an appreciable reduction in seedling survivorship near the tree. Similarly, at high fecundity and high seed dispersal distance, there could be a very high number of seeds throughout the simulation space, and again the effect of the pathogens is relatively low. As we can see from figure 3.4, low fecundity results in seedlings far from adult trees – pathogens can successfully infect and kill a large number of seeds at these densities. Finally, at intermediate distances, the combination of fecundity and seed dispersal distance creates a density gradient that most closely matches the spatial pattern of spores. This results in high seed mortality near the adult tree, and an increase in survival probability with increasing distance, with a peak at a distance outside the crown of the adult tree – in effect, a Janzen-Connell pattern. This is supported by our measurements of seedling recruitment patterns, in which moderate seed dispersal distances maintain Janzen-Connell effects in spite of high tree fecundities (Fig. 3.2).

3.2.2 The Prevention of Tree Saturation by Pathogens

Under the parameter combinations we applied to this model, the number of trees present in the system at equilibrium was determined by tree fecundity, seed dispersal distance, and pathozone radius (Fig. 3.5). The previously mentioned effect of intermediate-distance of seed dispersal limited tree population size when tree fecundity was greater than 20,000. At low fecundity, the pathozone radius reduced the equilibrium number of trees. Again, the seed dispersal distances above 8.3 meters and below 7.3 meters caused seed densities to be so high that pathogens could not effectively limit tree establishment. At moderate distances, pathogens were able to respond to seed densities and reduce tree growth. And at low tree fecundity, pathogens were able to severely limit the number of trees in the system.

Janzen-Connell patterns emerge in a plant system due to mortality by specialized natural enemies, and evidence suggests pathogens play an important role in creating Janzen-Connell patterns (Augspurger, 1983; Sarmiento et al., 2017; Liang et al., 2016; Bagchi et al., 2010). Our results provide indicators of plant responses to pathogens based on their life history. Pathogens resist satiation from high seed densities unlike insect natural enemies, instead being limited by gaps in seed density (Beckman et al., 2012), but in the majority of our simulations the landscape was saturated with trees within 500 seed dispersal seasons. Mortality due to pathogens in our model does not seem to be strong enough to limit populations in a way that would promote local coexistence with many of our parameter combinations. The factors that did allow Janzen-Connell patterns, seed dispersal distance and tree fecundity, are related to tree attributes and not pathogens, indicating that pathogens attributes are less important than pathogen presence in the system.

The discrepancy between our results, which show that pathogen attributes do not influence the development of Janzen-Connell patterns or tree population responses, and the expected influence of pathogens may be due to the influence of secondary seed dispersers and other natural enemies in natural systems which may alter the initial seed shadow prior to pathogen attack (Fricke et al., 2014; Bagchi et al., 2014), depending on their movement patterns (Mari et al., 2008). This would reduce the density of seeds

and potentially allow pathozone radius to have an influence at a higher level of tree fecundity. Scatter-hoarding rodents secondarily disperse seeds modifying the initial seed shadow (Jansen et al., 2004), dispersing seeds toward areas with low conspecific density (Hirsch et al., 2012), which can drastically change the ability of pathogens to affect seedling mortality (Beckman et al., 2012). Further research into systems with multiple natural enemies, including those with host-specific and generalist consumption patterns, is necessary to understand the full potential of pathogen natural enemies.

3.2.3 Pathogens Rely on Seeds for Dispersal and Population Growth

Many of our results indicate that pathogen patterns are largely moderated by tree fecundity and seed dispersal distance (Figs. 3.6, 3.7, 3.10) instead of pathogen attributes. We expected the ability of pathogens to disperse to play a much larger role in determining tree and pathogen population patterns, given the importance of pathogens' ability to track seed distributions established by Beckman et al. (2012). Indeed, based on the results of Muller-Landau and Adler (2007), we expected the relative dispersal distance of zoospores and seeds to influence seedling recruitment patterns more than were shown in our results. However, both pathogen dispersal distance and the ratio between seed and pathogen dispersal were only significant under specific combinations of other parameters, including pathogen-related parameters like pathozone radius and oospores produced per infected host (Figs. 3.2, 3.11).

This result may arise from the discrete spatial nature of the model. In the model, zoospores disperse between cells, but all zoospores have probabilistic interactions with all seeds in their cell, regardless of dispersal parameters. Therefore zoospores effectively have a uniformly distributed dispersal kernel across their cell with a maximum distance of $5\sqrt{2}$ meters. Such distances of zoospore dispersal are not unheard of, such as during flooding events or animal vectors (Ristaino and Gumpertz, 2000), but the assumption that this kind of dispersal is likely to occur omni-directionally more than once during a season, as this model implicitly does, may be extreme. Regardless, this attribute of the model means that the zoospore dispersal parameter only causes splits in the regression tree at unlikely distances of zoospore dispersal. For example, in figure 3.13 a split is created by zoospore dispersal at 6.5 meters, and in figure 3.11 zoospore dispersal creates

a split at 9.6 meters. Most of the zoospore dispersal parameter influence that would have caused splits in the regression trees has been overshadowed by the probabilistic infection of seedlings within the cell, which is uncontrolled by the zoospore dispersal parameter.

The zoospore dispersal parameter manages pathogen movement between cells, but it has minimal effects on the tree or pathogen populations themselves. Small zoospore dispersal distance reduces the number of spores that land in a neighboring cell, but large numbers of spores, driven by the number of hosts in the cell, more than make up the difference. The fact that zoospore dispersal distance does not split the regression trees more underscores the importance of infection to the pathogen's ability to influence a tree population. Pathozone radius and oospore fecundity were the most common pathogen attributes to cause splits in regression trees, both of which directly determine the ability of pathogens to infect hosts within the cell.

The results of Truscott et al. (2000) and Truscott et al. (1997) indicate that pathogen populations can be supported in a population of agricultural crops when only oospores ("primary infection") or zoospores ("secondary infection") are active. Our results support this conclusion, though the structure of zoospore dispersal creates a high potential zoospore infection rate inside the cells. If we were to change this attribute of the model, we may find a similar result, with the pathogen able to persist in the system with either zoospore or oospore infection only.

3.2.4 Pathogen Presence versus Attributes

The importance of tree attributes to determining both seed and pathogen patterns in the simulation space indicate that the presence of pathogens is their most influential attribute. Pathogen attributes did differentiate between Hubbell and McCanny patterns, but not Janzen-Connell patterns (Fig. 3.2).

However, the unimportance of pathogen attributes may be a result of model structure. Above a certain seed density, a cell's pathozone coverage reaches 100%, causing every spore to encounter and potentially infect a seed. Pathozone radius had no effect beyond this point. Pathogen fecundity had little effect, as the zoospores infecting hosts

within a cell were redundant with oospores, and even a small number of zoospores could colonize neighboring cells. The number of oospores per host influenced host infection, but also had an upper limit of effectiveness as the probability of infecting all the hosts in the cell approached 1 at high oospore populations.

The zoospore dispersal within the cells may also have contributed to the lack of influence of pathogens on seedling recruitment patterns. Zoospores dispersed across small subcells ($0.01m^2$), that were then overlain on the larger cells of trees ($25m^2$). This discrete partitioning of space allowed zoospores to disperse further than would be expected based on their mean dispersal distance. In future versions of the model, we will examine the influence of smaller cell sizes for trees or assume continuous space for tree dynamics to better reflect zoospore dispersal, allowing a more direct comparison between zoospore and oospore effects on the pathogen and tree population dynamics.

3.2.5 The Importance of Tree Fecundity

Our results indicate that tree fecundity was an important attribute of the response of a tree population to pathogen natural enemies. In other models, tree fecundity was not tested for its impact on seedling recruitment, but seedling dispersal distance was (Beckman et al., 2012; Muller-Landau and Adler, 2007). In our model, tree fecundity in combination with seed dispersal distance determined local seed densities. High tree fecundity values combined with high or low seed dispersal distances overwhelmed pathogen capabilities, while low fecundity values allowed pathogens to have a significant effect on seedling recruitment patterns.

3.2.6 Pathogens Tracking Hosts

Beckman et al. (2012) indicate that the ability of natural enemies to track seed dispersal is an important factor influencing seedling recruitment patterns. Our results indicate that the ability of pathogens to track seeds (Fig. 3.8) is primarily a result of oospores produced per infected host, and the pathozone radius. These parameters are among those we expected to influence the spatial relationship between seeds and trees, especially given the structure of zoospore dispersal in our model. A simulation utilizing a more realistic mechanism of zoospore dispersal within cells would likely demonstrate

the importance of zoospore dispersal in tracking seeds as well.

Our results did agree with those found by Beckman et al. (2012) in that many of the recruitment patterns observed indicated Janzen-Connell patterns, though significantly more of our simulations showed McCanny and Hubbell patterns. Neither study, however, measured the strength of the patterns observed (i.e. the steepness of the survivorship curve and/or the probability recruitment curve). A future study could include a measurement of the strength of the seedling recruitment patterns observed, which would more directly tie pathogen and tree attributes to the development of seedling recruitment patterns than the categorization algorithm used in this project.

3.2.7 Relative Dispersal Distance Between Hosts and Natural Enemies

Muller-Landau and Adler (2007), Nathan and Casagrandi (2004), and Mari et al. (2008) indicate that the relative dispersal distance between hosts and natural enemies influences the development of Janzen-Connell recruitment patterns. Beckman et al. (2012) also indicate that relative dispersal distance of seeds and pathogens may play a role in seedling recruitment patterns. The results presented here, however, do not provide support for the development of Janzen-Connell patterns by pathogens, instead identifying their role as differentiating between Hubbell and McCanny patterns. We see the importance of pathogen reproduction as well as tree fecundity and dispersal. However, this model's assumptions for discrete space for the trees and how this interacted with zoospore dispersal may have absorbed much of the effect of zoospore dispersal distance that would have been observed. With a different model structure, the relative dispersal distances of seeds and zoospores may have been an important explanatory variable in the regression trees, and our results would agree with those of Beckman et al. (2012) and Muller-Landau and Adler (2007).

3.2.8 Parameters for Higher Scale Models

There is some interest in using population and community scale models to inform which variables may be important to take into account for larger-scale environmental models (Corlett, 2011; examples: Mniszewski et al., 2014; Cilfone et al., 2015). The model presented here indicates that the attributes of the tree species are the most

influential in determining the tree population size and dynamics, and therefore should be included in a "higher-level" model. Pathogen presence seems to be more important than pathogen attributes, but oospores produced per host could be a useful parameter to include, as would pathozone radius. Other pathogen attributes which we examined were not shown to be significant, and should not be included as they would not justify the computational resources they would require.

The lack of conclusive results in regards to the role of zoospore dispersal is of particular concern. Changes in water availability due to climate change and deforestation could reduce species diversity in tropical forests via limitation of zoospore dispersal (Swinfield et al., 2012). Future research will focus on the role of zoospore dispersal in seedling recruitment patterns to determine if this is an important dynamic that should be included in larger-scale models.

Dormant oospore mortality did not play a significant role in the dynamics of the tree and pathogen populations and interactions. We hypothesized that oospore dormancy would be integral to pathogens' ability to impact seedling recruitment patterns. However, the dormant oospore mortality parameter only appeared in one of our regression trees (Fig. 3.11) and only applied at low tree fecundity. Intuitively, low tree fecundity makes dormancy more likely due to low seed densities. With a population of trees, however, even moderate tree fecundity would make it unlikely for spores to remain dormant for any appreciable length of time, limiting the impact of oospore dormancy on the system.

3.3 Conclusions

Tree fecundity, seed dispersal distance, and pathozone radius had the largest impact on seedling recruitment and pathogen effectiveness in our model, but we were unable to concretely determine the importance of zoospore dispersal distance. Seed dispersal attributes had the largest impact on tree population structure, but pathogen presence had an important influence on tree density and seedling recruitment. Further study will focus on the role of pathogen dispersal and measuring the strength of seedling recruitment patterns.

REFERENCES

Adler, F. R., and H. C. Muller-Landau. 2005. When do localized natural enemies increase species richness? Ecology Letters **8**:438–447.

Alden, K., M. Read, P. Andrews, J. Cosgrove, M. Coles, and J. Timmis, 2018. Simulation Parameter Analysis R Toolkit Application: 'spartan'. URL http://cran.r-project.org/package=spartan.

Armstrong, R. A. 1989. Competition, Seed Predation, and Species Coexistence. Journal of Theoretical Biology **141**:191–195.

Augspurger, C. K. 1983. Seed Dispersal of the Tropical Tree, *Platypodium Elegans*, and the Escape of its Seedlings from Fungal Pathogens. Ecology **71**:759–771.

Augspurger, C. K., 1990. Spatial patterns of damping-off disease during seedling recruitment in tropical forests. Chapter 9, pages 131–144 *in* J. J. Burdon and S. R. Leather, editors. Pests, Pathogens and Plant Communities. Blackwell Scientific Publications, Oxford.

Augspurger, C. K., and C. K. Kelly. 1984. Pathogen mortality of tropical tree seedlings: studies of the effects of dispersal distance, experimental seedling density, and light conditions. Oecologia **61**:211–217.

Augspurger, C. K., and K. Kitajima. 1992. Experimental Studies of Seedling Recruitment from Contrasting Seed Distributions. Ecology **73**:1270–1284.

Augspurger, C. K., and H. T. Wilkinson. 2007. Host specificity of pathogenic *Pythium* species: implications for tree species diversity. Biotropica **39**:702–708.

Babadoost, M., and C. Pavon. 2013. Survival of Oospores of Phytophthora capsici in Soil. Plant Disease **97**:1478–1483.

Bagchi, R., R. E. Gallery, S. Gripenberg, S. J. Gurr, L. Narayan, C. E. Addis, R. P. Freckleton, and O. T. Lewis. 2014. Pathogens and insect herbivores drive rainforest plant diversity and composition. Nature **506**:85–88.

Bagchi, R., T. Swinfield, R. E. Gallery, O. T. Lewis, S. Gripenberg, L. Narayan, and R. P. Freckleton. 2010. Testing the Janzen-Connell mechanism: Pathogens cause overcompensating density dependence in a tropical tree. Ecology Letters **13**:1262–1269.

Bailey, D. J., and C. A. Gilligan. 1999. Dynamics of primary and secondary infection in take-all epidemics. Phytopathology **89**:84–91.

Bailey, D. J., N. Paveley, C. Pillinger, J. Foulkes, J. Spink, and C. A. Gilligan. 2005. Epidemiology and chemical control of take-all on seminal and adventitious roots of wheat. Phytopathology **95**:62–68.

Beckman, N. G., C. Neuhauser, and H. C. Muller-Landau. 2012. The interacting effects of clumped seed dispersal and distance- and density-dependent mortality on seedling recruitment patterns. Journal of Ecology **100**:862–873.

Berish, C. W. 1981. Root biomass and surface area in three successional tropical forests. Canadian Journal of Forest Research **12**:699–704.

Bever, J. D., S. A. Mangan, and H. M. Alexander. 2015. Maintenance of Plant Species Diversity by Pathogens. Annual Review of Ecology, Evolution, and Systematics **46**:305–325.

Bohlman, S., and S. O'Brien. 2006. Allometry, adult stature and regeneration requirement of 65 tree species on Barro Colorado Island, Panama. Journal of Tropical Ecology **22**:123–136.

Bowers, J., G. Papayizas, and S. Johnston. 1990. Effect of soil temperature and soil water matric potential on the survival of Phytopthora capsici in natural soil. Plant Disease **74**:771–777.

Brassett, P. R., and C. A. Gilligan. 1988. A discrete probability model for polycyclic infection by soilborne plant parasites. New Phytologist **109**:183–191.

Bullock, J. M., L. Mallada González, R. Tamme, L. Götzenberger, S. M. White, M. Pärtel, and D. A. P. Hooftman. 2017. A synthesis of empirical plant dispersal kernels. Journal of Ecology **105**:6–19.

Chesson, P. 2000. Mechanisms of Maintenance of Species Diversity. Annual Review of Ecology and Systematics **31**:343–66.

Cilfone, N. A., D. E. Kirschner, and J. J. Linderman. 2015. Strategies for Efficient Numerical Implementation of Hybrid Multi-scale Agent-Based Models to Describe Biological Systems. Cellular and Molecular Bioengineering **8**:119–136.

Clark, J. S., M. Silman, R. Kern, E. Macklin, and J. HilleRisLambers. 1999. Seed Dispersal Near and Far: Patterns Across Temperate and Tropical Forests. Ecology **80**:1475–1494.

Comita, L. S., S. A. Queenborough, S. J. Murphy, J. L. Eck, K. Xu, M. Krishnadas, N. Beckman, and Y. Zhu. 2014. Testing predictions of the Janzen Connell hypothesis : a meta-analysis of experimental evidence for distance- and density-dependent seed and seedling survival. Journal of Ecology **102**:845–856.

Condit, R., R. Pérez, S. Lao, S. Aguilar, and S. P. Hubbell. 2017. Demographic trends and climate over 35 years in the Barro Colorado 50 ha plot. Forest Ecosystems **4**:1–13.

Connell, J. H., 1971. 1. Pages 298–312 *in* P. J. Den Boer and G. R. Gradwell, editors. Dynamics of Populations. Center for Agricultural Publishing and Documentation, Wageningen.

Corlett, R. T. 2011. Impacts of warming on tropical lowland rainforests. Trends in Ecology and Evolution **26**:606–613.

Delmas, C. E. L., I. D. Mazet, J. Jolivet, L. Delière, and F. Delmotte. 2014. Simultaneous quantification of sporangia and zoospores in a biotrophic oomycete with an automatic particle analyzer: Disentangling dispersal and infection potentials. Journal of Microbiological Methods **107**:169–175.

Fitt, B. D. L., P. H. Gregory, A. D. Todd, H. McCartney, and O. Macdonald. 1987. Spore Dispersal and Plant Disease Gradients: a Comparison between two Empirical Models. Journal of Phytopathology **118**:227–242.

French-Monar, R., J. Jones, M. Ozores-Hampton, and P. Roberts. 2007. Survival of Inoculum of Phtophthora casici in Soil Through Time Under Different Soil Treatments. Plant Disease **91**:593–598.

Fricke, E. C., J. J. Tewksbury, and H. S. Rogers. 2014. Multiple natural enemies cause distance-dependent mortality at the seed-to-seedling transition. Ecology Letters **17**:593–598.

Fricke, E. C., and S. J. Wright. 2016. The mechanical defence advantage of small seeds. Ecology Letters **19**:987–991.

Gallery, R. E., J. W. Dalling, and A. E. Arnold. 2007. Diversity, host affinity, and distribution of seed-infecting fungi: A case study with *Cecropia*. Ecology **88**:582–588.

García-Guzmán, G., and E. Morales. 2007. Life-History Strategies of Plant Pathogens: Distribution Patterns and Phylogenetic Analysis. Ecology **88**:589–596.

Gilligan, C. A. 1985. Probability models for host infection by soilborne fungi. Phytopathology **75**:61–67.

Gilligan, C. A., and D. J. Bailey. 1997. Components of pathozone behaviour. New Phytologist **135**:475–490.

Grove, G., L. Madden, and M. Ellis. 1985. Influence of temperature and wetness duration on sporulation of *Phytophthora cactorum* on infested strawberry fruit. Phytopathology **75**:700–703.

Heungens, K., and J. L. Parke. 2000. Zoospore homing and infection events: Effects of the biocontrol bacterium *Burkholderia cepacia* AMMDR1 on two oomycete pathogens of pea (*Pisum sativum* L.). Applied and Environmental Microbiology **66**:5192–5200.

Hirsch, B. T., R. Kays, V. E. Pereira, and P. A. Jansen. 2012. Directed seed dispersal towards areas with low conspecific tree density by a scatter-hoarding rodent. Ecology Letters **15**:1423–1429.

Hubbell, S. P. 1980. Seed predation and the coexistence of tree species in tropical forests. Oikos **35**:214–229.

Jansen, P. A., F. Bongers, and L. Hemerik. 2004. Seed mass and mast seeding enhance dispersal by a neotropical scatter-hoarding rodent. Ecological Monographs **74**:569–589.

Janzen, D. H. 1970. Herbivores and the Number of Tree Species in Tropical Forests. The American Naturalist **104**:501–528.

Judelson, H. S., and F. A. Blanco. 2005. The spores of *Phytophthora*: Weapons of the plant destroyer. Nature Reviews Microbiology **3**:47–58.

Konno, M., S. Iwamoto, and K. Seiwa. 2011. Specialization of a fungal pathogen on host tree species in a cross-inoculation experiment. Journal of Ecology **99**:1394–1401.

Latijnhouwers, M., P. J. G. M. De Wit, and F. Govers. 2003. Oomycetes and fungi: Similar weaponry to attack plants. Trends in Microbiology **11**:462–469.

Liang, M., X. Liu, G. S. Gilbert, Y. Zheng, S. Luo, F. Huang, and S. Yu. 2016. Adult trees cause density-dependent mortality in conspecific seedlings by regulating the frequency of pathogenic soil fungi. Ecology Letters **19**:1448–1456.

Liu, X., M. Liang, R. S. Etienne, Y. Wang, C. Staehelin, and S. Yu. 2012. Experimental evidence for a phylogenetic Janzen-Connell effect in a subtropical forest. Ecology Letters **15**:111–118.

Liu, Y., and F. He. 2019. Incorporating the disease triangle framework for testing the effect of soilborne pathogens on tree species diversity. Functional Ecology **33**:1211–1222.

Mari, L., R. Casagrandi, M. Gatto, T. Avgar, and R. Nathan. 2008. Movement Strategies of Seed Predators as Determinants of Plant Recruitment Patterns. The American Naturalist **172**:694–711.

Martin, F. N., and J. E. Loper. 1999. Soilborne Plant Diseases Caused by Pythium spp.: Ecology, Epidemiology, and Prospects for Biological Control. Critical Reviews in Plant Science **18**:111–181.

McCanny, S. J. 1985. Alternatives in parent-offspring relationships in plants. Oikos **45**:148–149.

Mniszewski, S. M., C. A. Manore, C. Bryan, S. Y. Del Valle, and D. Roberts. 2014. Towards a Hybrid Agent-based Model for Mosquito Borne Disease. Summer Computer Simulation Conference 2014 page 10.

Mordecai, E. A. 2011. Pathogen impacts on plant communities: unifying theory, concepts, and empirical work. Ecological Monographs **81**:429–441.

Muller-Landau, H. C., and F. R. Adler, 2007. How Seed Dispersal Affects Interactions with Specialized Natural Enemies and their Contribution to the Maintenance of Diversity. Chapter 18, pages 407–426 *in* Seed Dispersal Theory Applications in a Changing World. CABI.

Muller-Landau, H. C., R. S. Condit, J. Chave, S. C. Thomas, S. A. Bohlman, S. Bunyavejchewin, S. Davies, R. Foster, S. Gunatilleke, N. Gunatilleke, K. E. Harms, T. Hart, S. P. Hubbell, A. Itoh, A. R. Kassim, J. V. LaFrankie, H. S. Lee, E. Losos, J. R. Makana, T. Ohkubo, R. Sukumar, I. F. Sun, M. N. Nur Supardi, S. Tan, J. Thompson, R. Valencia, G. V. Muñoz, C. Wills, T. Yamakura, G. Chuyong, H. S. Dattaraja, S. Esufali, P. Hall, C. Hernandez, D. Kenfack, S. Kiratiprayoon, H. S. Suresh, D. Thomas, M. I. Vallejo, and P. Ashton. 2006. Testing metabolic ecology theory for allometric scaling of tree size, growth and mortality in tropical forests. Ecology Letters **9**:575–588.

Muller-Landau, H. C., S. J. Wright, O. Calderón, R. Condit, and S. P. Hubbell. 2008. Interspecific variation in primary seed dispersal in a tropical forest. Journal of Ecology **96**:653–667.

Murphy, S. J., T. Wiegand, and L. S. Comita. 2017. Distance-dependent seedling mortality and long-term spacing dynamics in a neotropical forest community. Ecology Letters **20**:1469–1478.

Nathan, R., and R. Casagrandi. 2004. A simple mechanistic model of seed dispersal, predation and plant establishment: Janzen-Connell and beyond. Journal of Ecology **92**:733–746.

Nathan, R., E. K. Klein, J. J. Robledo-Arnuncio, and E. Revilla, 2012. Dispersal kernels: review. Chapter 15 *in* Dispersal Ecology and Evolution. Oxford University Press.

Neher, D. A., C. K. Augspurger, and H. T. Wilkinson. 1987. Influence of age structure of plant populations on damping-off epidemics. Oecologia **74**:419–424.

O'Brien, S. T., S. P. Hubbell, P. Spiro, R. Condit, and R. B. Foster. 1995. Diameter, height, crown, and age relationships in eight neotropical tree species. Ecology **76**:1926–1939.

Rekah, Y., D. Shtienberg, and J. Katan. 2007. Spatial Distribution and Temporal Development of Fusarium Crown and Root Rot of Tomato and Pathogen Dissemination in Field Soil. Phytopathology **89**:831–839.

Ristaino, J. B., and M. L. Gumpertz. 2000. New Frontiers in the Study of Dispersal and Spatial Analysis of Epidemics Caused by Sepecies in the Genus *Phytophthora*. Annual Reviews of Phytopathology **38**:541–576.

Russo, S. E., S. Portnoy, and C. K. Augspurger. 2006. Incorporating Animal Behavior into Seed Dispersal Models: Implications for Seed Shadows. Ecology **87**:3160–3174.

Sarmiento, C., P.-C. Zalamea, J. W. Dalling, A. S. Davis, S. M. Stump, J. M. U'Ren, and A. E. Arnold. 2017. Soilborne fungi have host affinity and host-specific effects on seed germination and survival in a lowland tropical forest. Proceedings of the National Academy of Sciences **114**:11458–11463.

Sedio, B. E., and A. M. Ostling. 2013. How specialised must natural enemies be to facilitate coexistence among plants? Ecology Letters **16**:995–1003.

Souza, F. M., G. A. D. C. Franco, and R. M. Callaway. 2013. Strong distance-dependent effects for a spatially aggregated tropical species. Plant Ecology **214**:545–555.

Stanghellini, M., and J. Hancock. 1971. The sporangium of *Pythium ultimum* as a survival structure in soil. Phytopathology **61**:157–164.

Swinfield, T., O. T. Lewis, R. Bagchi, and R. P. Freckleton. 2012. Consequences of changing rainfall for fungal pathogen-induced mortality in tropical tree seedlings. Ecology and Evolution **2**:1408–1413.

Therneau, T., and B. Atkinson, 2018. rpart: Recursive Partitioning and Regression Trees. URL https://cran.r-project.org/package=rpart.

Timmer, L., S. Zitko, T. Gottwald, and J. Graham. 2000. Phytophthora Brown Rot of Citrus: Temperature and Moisture Effects on Infection, Sporangium Production, and Dispersal. Plant Disease **84**:175–163.

Truscott, J., C. Webb, and C. Gilligan. 1997. Asymptotic Analysis of an Epidemic Model with Primary and Secondary Infection. Bulletin of Mathematical Biology **59**:1101–1123.

Truscott, J. E., C. R. Webb, and C. A. Gilligan. 2000. Quantitative Analysis and Model Simplification of an Epidemic Model with Primary and Secondary Infection. Bulletin of Mathematical Biology **62**:377–393.

Widmer, T. 2009. Infective Potential of Sporangia and Zoospores of *Phytophthora ramorum*. Plant Disease **93**:30–35.

Wright, S. J. 2002. Plant diversity in tropical forests: a review of mechanisms of species coexistence. Oecologia **130**:1–14.

APPENDIX

Most parameters were taken directly from the literature, from models focused on similar problems or empirical research that measured certain aspects of pathogen lifecycles.

Dormant Oospore Mortality ($0.75 < \sigma < 0.95$): Dormant oospore mortality was adapted from Beckman et al. (2012), but allowed to vary within a given range to test the effect of dormant oospore mortality. However, the minimum value was kept high, at 0.75, in order to approximate empirically observed ranges (French-Monar et al., 2007; Bowers et al., 1990), while allowing enough variation to get a comprehensive view of the effect of dormant oospore mortality.

Pathozone Radius ($0.001 < r < 0.1$m): Oospore pathozone radius is roughly 10 mm (Stanghellini and Hancock, 1971) while zoospores have been shown to infect hosts within short distances, from 6 to 15 mm (Fitt et al., 1987), and upwards of 30 mm (Heungens and Parke, 2000). We made the simplifying assumption that the pathozone radii for zoospores and oospores were the same, as the effect of the difference between them was not of central interest to this project.

Time Steps t in f ($c = 4$): The number of zoospore dispersal events between each seed dispersal was determined by incorporating the limited season of seedling mortality (Augspurger, 1983) with the timing of a complete pathogen lifecycle, which ranges from less than a day to sometimes as much as a week (Judelson and Blanco, 2005; Brassett and Gilligan, 1988). The value of $c = 4$ matches with that used by Beckman et al. (2012).

Zoospores Produced per Active Oospore ($2 < \mu < 15$): The number of zoospores per empty oospore was observed to be between 2.8 and 10.1 by Delmas et al. (2014). Accordingly, the number of zoospores per oospore in our model was varied between 2 and 15 to capture this range as well as additional variability in zoospore production due to differences in oomycete species or environmental conditions that may affect zoospore production directly (Judelson and Blanco, 2005) and via oospore production (Heungens and Parke, 2000; Timmer et al., 2000; Grove et al., 1985).

Oospores per Infected Host ($1000 < \omega < 1,500,000$): Oospores produced per infected host depends on the size of a seed. Empirical research indicates that up to 660 oospores per square millimeter of host surface area is possible (Timmer et al., 2000; Grove et al., 1985). Using seed size data from Fricke and Wright (2016) and the Thomsen approximation to the surface area of an ellipsoid, we were able to calculate the range of seed surface areas for seeds measured on Barro Colorado Island, Panama. This calculation resulted in an estimated range of 74 to 95,700 square millimeters of surface area and an estimated range of oospores produced per seed of 48,956 and 63,162,489 oospores at this maximum coverage rate. However, the production of oospores on the surface of the host could be much smaller due to environmental conditions, pathogen traits, plant traits, and their interactions. In our model, we explore a large range of oospore production, over three orders of magnitude.

Average Zoospore Dispersal Distance ($0.01 < q < 10$m): Zoospores have been found to disperse varying distances depending on conditions. When relying only on soil water, they are limited in range as the only form of locomotion is from their own flagella – around 6 to 15 mm (Fitt et al., 1987). In other cases, flowing water through and over the soil can carry zoospores much longer distances, as can splashing surface water – in these cases, 0.8 to 13 m dispersal has been recorded (Fitt et al., 1987). We varied zoospore dispersal distance throughout the ranges measured for these two mechanisms to capture their effects.

Infectivity Constant ($\nu = 0.01$): As described in Appendix S1 of Beckman et al. (2012), infectivity was determined from published empirical data (Martin and Loper, 1999; Widmer, 2009) as $-log$(probability that a host remains susceptible)/(number of hosts) to be between 0.001 and 0.04.

Root Pathozone Coverage (100%): Roots are assumed to cover the entire spatial cell where a tree is found, which is supported by studies of root density under trees (Berish, 1981).

Initial Tree Population (30): The initial tree population for the model was chosen to be a small number from which the population could grow without significant effect of initial tree location on future tree spatial patterns.

Initial Infected Tree Proportion (0.3): The proportion of initially infected trees was chosen to create a population of pathogens in the system sufficiently large to have a presence.

Infected Seed Mortality ($\delta = 0.9$): Infected seed mortality was selected to be very high, based on the studies reviewed by Martin and Loper (1999) which showed that young seedlings have a high mortality rate. Seedlings have been shown to have the highest mortality between 2 and 7 weeks of germination (Augspurger, 1983).

Adult Tree Mortality ($\gamma = 0.0225$): Adult tree mortality was based on data taken from Barro Colorado Island for adult tree mortality (Condit et al., 2017).

Seed Dispersal Shape ($b = 3$): The seed dispersal shape parameter was matched to that used by other studies, such as Beckman et al. (2012), Muller-Landau et al. (2008), and Clark et al. (1999).

Average Seed Dispersal Distance ($-0.9 < a < 5.54$): Average seed dispersal distance for trees on BCI have a range of roughly 5 to 125 meters (Muller-Landau et al., 2008). The desired distance in meters was converted to the scale parameter used by the 2Dt dispersal kernel, with values between -0.9 and 5.54.

Seeds per Dispersal per Tree ($1,000 < j < 250,000$): Tropical tree fecundity ranges from 0.0438 to 1764 per square centimeter of basal area, depending on the size of the seeds (Clark et al., 1999; Muller-Landau et al., 2008). With a uniform canopy size of 25 square meters for all reproductive trees in our model, we would expect between 10950 and 441 million seeds per tree. An intermediate range of 1,000 to 250,000 was selected as the impact of seed dispersal was not a primary focus for this study, and this density of seed production matches that used in Beckman et al. (2012).

Background Seedling Mortality (0.5): Seedling mortality independent of mortality due to pathogen infection was matched with that used by Beckman et al., 2012 to include background rates of seedling mortality due to environmental conditions not explicitly modeled here.

Spatial Cell Area ($\epsilon = 25x25\mathbf{m}^2$): The area of spatial cells was set to the size of a typical tropical tree canopy for a single adult individual (O'Brien et al., 1995; Bohlman

and O'Brien, 2006; Muller-Landau et al., 2006) and matches the canopy size used in Beckman et al. (2012).

Spatial Sub-Cell Area (0.01x0.01 m): The size of spatial sub-cells was selected as approximately the range over which most seed-zoospore interactions would be taking place while allowing for reasonably efficient processing.